Am J Physiol Gastrointest Liver Physiol
279: G1265–G1273, 2000.

Functional properties of transfected human DMT1 iron transporter

MARK T. WORTHINGTON, LAUREN BROWNE, EMILY H. BATTLE, AND ROGER QI LUO
Digestive Health Research Center, Division of Gastroenterology and Hepatology, University of Virginia Health Sciences Center, Charlottesville, Virginia 22908-0708

Received 1 November 1999; accepted in final form 30 June 2000

Worthington, Mark T., Lauren Browne, Emily H. Battle, and Roger Qi Luo. Functional properties of transfected human DMT1 iron transporter. *Am J Physiol Gastrointest Liver Physiol* 279: G1265–G1273, 2000.—Recently, mutation of the *DMT1* gene has been discovered to cause ineffective intestinal iron uptake and abnormal body iron metabolism in the anemic Belgrade rat and *mk* mouse. DMT1 transports first-series transition metals, but only iron turns on an inward proton current. The process of iron transport was studied by transfection of human DMT1 into the COS-7 cell line. Native and epitope-tagged human DMT1 led to increased iron uptake. The human gene with the Belgrade rat mutation was found to have one-fifth of the activity of the wild-type protein. The pH optimum of human DMT1 iron uptake was 6.75, which is equivalent to the pH of the duodenal brush border. The transporter demonstrates uptake without saturation from 0 to 50 μM iron, recapitulating earlier studies of isolated intestinal enterocytes. Diethylpyrocarbonate inhibition of iron uptake in DMT1-transfected cells suggests a functional role for histidine residues. Finally, a model is presented that incorporates the selectivity of the DMT1 transporter for transition metals and a potential role for the inward proton current.

iron uptake; intestinal iron transporter

THE CLINICAL IMPORTANCE of iron uptake and utilization has long been recognized. Iron deficiency anemia, originally described by Hippocrates, affects millions worldwide. The hereditary iron-overload disease hemochromatosis, described by Trousseau in 1865, affects between 1 in 200 and 1 in 400 individuals in North America. Since the body lacks an effective method for excreting excess iron, increased intestinal uptake and transfer lead to increased body stores and end-organ damage, such as diabetes, cirrhosis, liver cancer, and arthritis. The mutation that causes hemochromatosis leads to increased expression of DMT1, a ubiquitous transmembrane protein, the expression of which is upregulated in the duodenum in iron deficiency (13, 15, 44). The product of this gene is required to transport dietary iron(II), in addition to a variety of other divalent first-series transition metal minerals, such as zinc, manganese, and copper. A mutation in rat and mouse *DMT1* leads to anemia, with defects in iron, manganese, and zinc metabolism (7, 12, 32), although the effect on the human protein is unknown.

The probability that DMT1 is the major intestinal iron transporter is intriguing, especially given the previous studies of enterocytes and inorganic iron uptake. Several studies using isolated enterocytes reported linear uptake of inorganic iron with increasing concentration, suggesting a process of facilitated transport that did not saturate under the conditions studied (11, 33, 36). This is not unlike other intestinal transporters that have a predominant facilitated diffusional component (30). Initial *Xenopus* oocyte microinjection studies of rat DMT1 revealed that iron binding is associated with an inward proton current that is activated at low iron concentrations [Michaelis-Menten constant (K_m) = 2 μM] but approaches saturation at ~10 μM (15). This proton current also increases from pH 7.5 to pH 5.5, suggesting that the lower pH might represent the transporter's optimum, as defined by the proton current. Previous studies have established the pH of the normal human duodenal mucosa to be 6.74 ± 0.15, a 16-fold lower proton concentration than pH 5.5 (25). The pH optima and affinity for substrate (K_m) of enzymes and transporters reflect the typical conditions of protein function and substrate concentration, respectively (4, 35). Thus the duodenum does not appear to be at the transporter's pH optimum or to have kinetic properties similar to those of the recombinant protein, leading to questions regarding its suitability as the major intestinal iron transporter. Whether the proton current in DMT1 represents the global process of iron uptake is unknown. We used a system of mammalian cell transfections to explore the properties of human DMT1 as the candidate intestinal iron transporter.

MATERIALS AND METHODS

COS-7 cells. COS-7 cells were obtained from the American Type Culture Collection and cultured in high-glucose DMEM containing 1 mM MEM-sodium pyruvate, 0.21% sodium bicarbonate, 10% fetal bovine serum, and 0.1 mM MEM-nonessential amino acid solution (all from Life Technologies) at 37°C with 5% CO_2 and ambient O_2. Standard tissue culture methods were used throughout the experiments.

Address for reprint requests and other correspondence: M. T. Worthington, University of Virginia Health System, PO Box 800708, Charlottesville, VA 22908-0708 (E-mail: mtw3p@virginia.edu).

The costs of publication of this article were defrayed in part by the payment of page charges. The article must therefore be hereby marked "*advertisement*" in accordance with 18 U.S.C. Section 1734 solely to indicate this fact.

Cloning of the human IRE form of DMT1 and construction of derivatives. The human *DMT1* gene was amplified from a commercial human cDNA library by 5′-rapid amplification of cDNA ends (Marathon RACE cDNA, Clontech) using the PCR and the 5′-primer from the kit, which includes a *Not* I site. The distal primer is CGG GGT ACC AAA CAC ACT GGC TCT GAT GGC TAC C. This second primer introduces a unique *Kpn* I restriction site 3′ to the native stop codon of the gene for cloning. For the 3′-epitope tag, amplification was performed with a primer that removes the stop codon and adds additional restriction sites (AAT GGG TAC CAG ATC TAA AGC TTA ACG TAT CCT CTG GTG GCT TCT TCT GTC AGC). The 3′ *T7* gene 10-tag sequence (Met-Ala-Ser-Met-Thr-Gly-Gly-Gln-Gln-Met-Gly) was then cloned as a pair of complementary phosphorylated oligonucleotides after restriction digestion of the plasmid with *Hin*d III and *Kpn* I (AGC TTG CAG CAG CCA TGG CAT GCA TGA CTG GAG GTC AGC AGA TGG CTG CGC TTT AAG GTA C; CTT AAA GCG CAG CCA TCT GCT GAC CTC CAG TCA TGC ATG CCA TGG CTG CTG CA). The G185R mutant was created by PCR with the 3′ primer using a 5′-mutant oligonucleotide that overlaps the native *Eco*R I site of the gene (GGA AGA ATT CCT CTG TGG GGT CGC GTT CTC ATC ACC ATT G). This construct was digested with *Eco*R I and *Xba* I and then reconstructed to form a COOH-terminal epitope-tagged DMT1 in our expression vector that differed only at *codon 185*.

Our initial experiments suggested that the complete coding region of the human DMT1 was toxic to DH5α *Escherichia coli* when cloned into a commercial high-copy mammalian expression vector (pBK-CMV, Stratagene). This effect apparently was not due to the iron concentration of the bacterial media, inasmuch as M9 medium without supplemental iron showed the same effect. The precise reason for the DMT1 toxicity in bacteria was not pursued further. After a number of unsuccessful attempts to make a high-copy DMT1 expression plasmid in other vectors, we modified an older, lower-copy mammalian expression plasmid that allowed us to proceed with transfection experiments. The parent expression plasmid pMW92 was constructed by cutting the simian virus 40 (SV40) early promoter expression plasmid pSGVP (29) with *Hin*d III and *Eco*R I to release the Gal4/VP16 insert and then ligating in overlapping oligonucleotides (AGC TTG TCG ACC AAT TGG CGG CCG CGG ATC CGA ATT CCC ATG GTA CC and AAT TGG TAC CAT GGG AAT TCG GAT CCG CGG CCG CCA ATT GGT CGA CA) to create a new multiple cloning site. This plasmid drives expression from the SV40 early promoter and has the SV40 polyadenylation site to improve message stability. All transfection experiments use this plasmid or a derivative containing the native DMT1 coding region, the COOH-terminal epitope-tagged protein, or G185R mutant COOH-terminal epitope-tagged protein.

Standard molecular biology practices were used throughout the experiments. Nucleobond Maxiprep low-copy plasmid purification kits (Clontech, Palo Alto, CA) were used to purify plasmid DNA for subcloning, transfections, and sequencing. Sequencing was performed at the University of Virginia Biomolecular Research Facility on a Perkin-Elmer ABI 377 sequencer with standard and custom primers. The integrity of each sequence was verified with primers on both strands, with at least twofold redundancy per base pair.

Transfections. COS-7 cells were transfected with Superfect reagent (Qiagen, Chatsworth, CA) using the manufacturer's protocol for optimization and ~60,000 cells in each well of a 24-well tissue culture dish. The total amount of DNA (0.72 μg) was kept constant. For the initial experiment to verify a functional DMT1 cDNA, no epitope tag was used. Subsequent experiments used the *T7* gene 10 epitope-tagged plasmids to verify protein expression after the kinetics of the two constructs were found to be comparable. Each condition of an experiment was performed in triplicate, and each experiment was repeated at least three times.

Iron(II) uptake. Iron uptake was measured 16–24 h after transfection using a standard method with radioactive iron and ascorbic acid (2): $^{55}FeCl_3$ is added to 1 mM ascorbic acid in water, the sample is incubated at room temperature for 15 min, and then the mixture is added to iron uptake buffer, which is similar to standard PBS solutions, except HEPES buffer is substituted for phosphate to avoid metal interactions (50 mM HEPES, 130 mM NaCl, 10 mM KCl, 1 mM $CaCl_2$, and 1 mM $MgSO_4$). Initial experiments were performed at pH 7.4 in this buffer. The pH determination experiments used the same salt and ascorbate concentrations, but a mixture of HEPES and MES extended the buffering capacity from pH 5.5 to 7.5. HEPES and MES were employed to avoid chelation and solubility problems encountered with metals in phosphate or Tris buffers (21). Once the pH optimum was determined to be 6.75, the diethylpyrocarbonate (DEPC) experiments were performed at this pH in the HEPES-MES buffer system. An ancillary benefit is that pH <7.2 has been shown to be more resistant to air oxidation in the ferrous-ascorbate electrocouple (10), although our linear uptake over a period of several hours suggests that this was not a major factor.

An ascorbate concentration of 1 mM was used because of its involvement in previous studies of inorganic iron uptake (2, 16) and because enterocyte cell lines have been shown to take up more inorganic iron as the ascorbate concentrations were increased to 1 mM (16). For the concentration assay in Fig. 3, radioactive and freshly dissolved nonradioactive iron(II) was mixed before the addition of 1 mM ascorbic acid at the highest concentrations, and the results were calculated for the specific activity of the metal. The solubility of the solutions over the concentration range was verified by comparing aliquots of the uptake solutions placed immediately in scintillation fluid with those incubated without cells for 2 h at 37°C. These were centrifuged at 21,000 *g* for 20 min, and the supernatant was added to scintillation fluid for counting. No significant differences in solubility were seen with or without the incubation.

In each experiment, 1 ml of the reduced, radioactive iron uptake buffer was added to each well, and the cells were incubated at 37°C and then washed three times with iron uptake buffer. An excess of unlabeled iron (100 μM in uptake buffer) was added to the first wash. Cells were then dissolved in lysis buffer (1% SDS, 1 mM EDTA, 100 μg/ml phenylmethylsulfonyl fluoride), and the protein concentration was determined using the Bio-Rad DC protein assay. Protein-normalized aliquots of the lysate were added to scintillation cocktail and counted using the open channel on a Beckman LS 6000-TA and Western blotting. Chemiluminescent Western blotting was performed on polyvinylidene difluoride membranes (Bio-Rad) using a commercial anti-T7 tag antibody/alkaline phosphatase conjugate (Novagen) and developed using CPD-Star (NEN) according to the manufacturer's protocol. Results are expressed as uptake normalized to total protein in the lysate. The molecular weight of DMT1 on Western blot was calculated using scanned images and the program NIH Image (26, 34).

DEPC treatment. Sealed DEPC ampoules (Sigma Chemical) were opened immediately before use and serially diluted in ice-cold PBS (Life Technologies) following an established method (31). All DEPC solutions were kept on ice before

incubation on the cells. The cell culture dishes were incubated with these solutions for 15 min at ambient temperature. A parallel non-DEPC control incubation was performed in PBS alone. Nonradioactive $FeCl_2$ and radioactive uptake solutions were freshly prepared before the incubation. After incubation, the cells were washed three times with our uptake buffer, pH 6.75, and then incubated with radioactive iron in uptake buffer for 2 h. For the nonradioactive iron preincubations, the iron was added to the PBS solutions because of uncertainty about the reactivity of DEPC to the HEPES-MES buffer. These were washed with the HEPES-MES uptake buffer before the addition of isotope.

Statistics. SE and ANOVA were calculated using the software StatView512$^+$ on a Macintosh G3 computer. ANOVA results were considered valid if Fisher's protected least significant difference test and Scheffé's F test were statistically significant at $P < 0.05$.

RESULTS

Linear uptake of iron in response to increasing DMT1 gene dosage. Our human DMT1 expression plasmid was transfected into the COS-7 cell line as an increasing proportion of DNA in the transfection experiment. Total DNA was kept constant by using the vector without insert. The results (Fig. 1) demonstrate linearly increasing iron uptake in response to an increasing concentration of DMT1 expression plasmid.

A COOH-terminal epitope-tagged protein functions like native human DMT1 and is useful for verifying protein expression. An epitope-tagged protein allows verification of comparable protein expression for each well. A COOH-terminal epitope-tagged DMT1 expression vector was created using the *T7* gene 10 epitope that was otherwise equivalent to our native DMT1 plasmid. This was done to verify that the transgenic protein was expressed. Lysates from mock-transfected, native DMT1-transfected, and COOH-terminal epitope tag-transfected COS-7 cells were normalized to protein concentration, resolved by SDS-PAGE, and blotted to polyvinylidene difluoride membrane for Western blotting. As seen in Fig. 2*A*, a band of the human DMT1 is seen only in the epitope-tagged protein lanes at a predicted molecular mass of 64 kDa (18). This compares favorably with the previously observed masses of 64 and 66 kDa for human DMT1 by PAGE (18, 38). Subsequent experiments have confirmed that the amount of immunoreactive tagged DMT1 protein is comparable between wells when normalized to total protein (not shown).

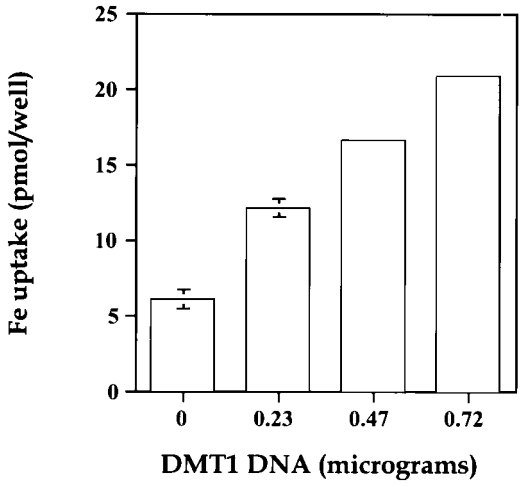

Fig. 1. Iron uptake by DMT1-transfected cells is dose responsive. COS-7 cells (60,000 cells/well, 24-well plate) were transfected in triplicate with an increasing proportion of DMT1-containing plasmid, from 0 to 100%. Total expression plasmid DNA content was kept constant at 0.72 μg with the vector alone. Iron uptake was measured 24 h after transfection with 1 μM radioactive iron at pH 7.4 in a 4-h incubation. After cells were washed once with cold iron in uptake buffer and twice with uptake buffer alone, they were lysed, and radioactive iron was measured. Error bars, SE; SE bars that are not visible are smaller than the graphic.

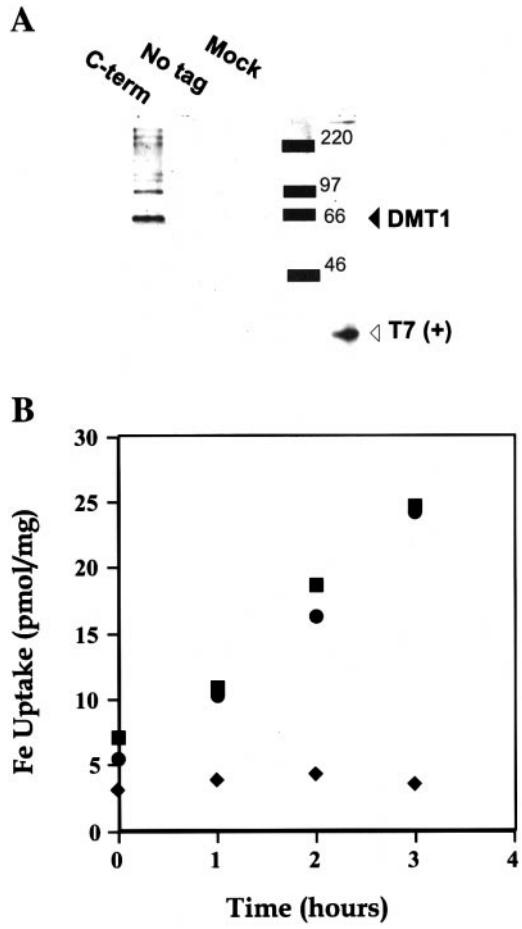

Fig. 2. Native and COOH-terminal epitope-tagged DMT1 are expressed and transport iron. COS-7 cells were transfected with vector alone, native DMT1, or DMT1 fused to a COOH-terminal T7 epitope tag. *A*: a commercial anti-T7 antibody is used to identify the epitope-tagged protein by Western blotting. Cellular protein lysates (20 μg/lane) of a Tris-glycine-SDS protein were electroblotted to polyvinylidene difluoride membrane and developed using a chemiluminescent protocol. The DMT1 epitope-tagged band is seen at 64 kDa (solid arrowhead) only in the COOH-terminal-tagged (C-term) protein lane, which correlates well with the published size of the human protein (18, 38). A commercial T7 positive control is also shown (open arrowhead). *B*: triplicate wells were transfected with mock (◆), native DMT1 (●), and epitope-tagged DMT1 plasmids (■), and 2 μM iron uptake studies were performed at pH 7.4. Both DMT1 plasmids lead to increased iron uptake with comparable kinetics, but the predicted DMT1 band is seen only in the epitope-tagged lanes. This epitope-tagged plasmid was used for all subsequent studies.

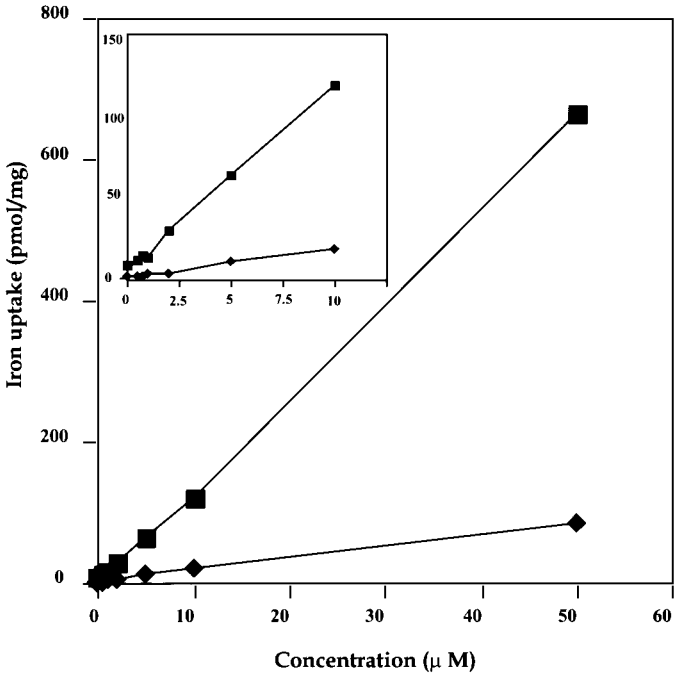

Fig. 3. Concentration dependence of iron uptake by transfected COS-7 cells. Uptake experiments were performed using DMT1-transfected (■) and mock-transfected (◆) cells at increasing concentrations of iron from 0–50 μM in a 2-h incubation at pH 7.4. *Inset*: the same data over 0–10 μM. In every condition, the error bars (SE) are smaller than the graphic.

The kinetics of COOH-terminal-tagged DMT1 were evaluated to determine whether this plasmid could be used in time-course experiments. Equivalent wells of COS-7 cells were transfected with the same amount of native, COOH-terminal-tagged, or mock DNA, and uptake experiments were repeated. The two DMT1 uptake curves were comparable over the 0- to 3-h time course of the experiment (Fig. 2*B*). Subsequent experiments were performed with the COOH-terminal epitope-tagged DMT1 plasmid. This was done to validate comparable expression levels of the protein in a variety of experimental conditions.

Concentration dependence of iron uptake by transfected DMT1. Older studies of inorganic iron uptake in isolated enterocytes suggested that iron uptake was linear over a broad concentration range (11, 33, 36). This is in distinction to the previous studies of DMT1 in *Xenopus* oocytes that described a saturable inward proton current, although the exact relationship between the proton current and iron transport has not been determined. If the iron uptake and proton influx have a fixed stoichiometry, this raises questions regarding the role of DMT1 as the major intestinal iron transporter. Whether DMT1 has properties similar to those reported in older studies of enterocytes was explored in our transfection system by varying the concentration of iron in the assay from 0 to 50 μM in a 2-h incubation at pH 7.4. The results (Fig. 3) show that DMT1 uptake is linear across this entire concentration range, analogous to earlier studies in isolated enterocytes. In addition to confirming the functional suitability of DMT1 as the candidate intestinal iron transporter, the results suggest that the kinetics of the inward proton current do not adequately model the entire process of iron uptake by this protein.

The human G185R mutation is expressed comparably to DMT1 in COS-7 cells and shows defective iron uptake. A naturally occurring DMT1 mutation is present in the anemic Belgrade rat and *mk* mouse (37), with global defects in iron utilization. The rat, mouse, and human DMT1 proteins are highly conserved (19). Initial studies of DMT1 in HEK-293 cells suggested that the lower uptake by the G185R mutant than by the native protein was a combined effect of lower protein expression and defective protein function (37). Since COS-7 cells can episomally amplify plasmids with the SV40 origin of replication, we hypothesized that expression in this cell line would lead to comparable protein levels and, thus, allow this question of protein dysfunction to be answered more directly. All the plasmids used for this study contain the SV40 origin of replication as part of the SV40 early promoter (29).

Figure 4*A* shows that the amounts of protein expression of the G185R mutant are comparable to a simi-

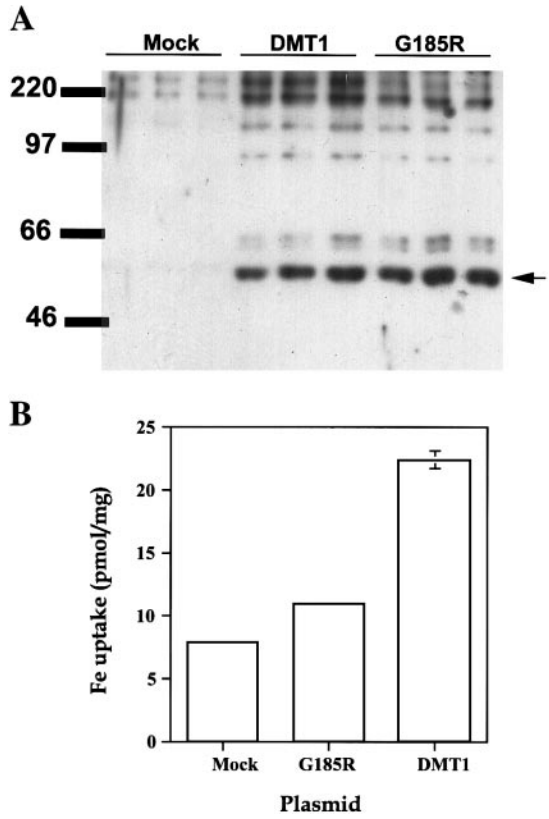

Fig. 4. Human G185R mutation is expressed comparably to the native DMT1 protein in COS-7 cells and impairs DMT1 function. *A*: mock-transfected, COOH-terminal epitope-tagged DMT1-transfected (C-term), and epitope-tagged human G185R-transfected cell lysates were evaluated by Western blotting. Protein lysate (20 μg/lane) was loaded from triplicate wells for each plasmid. *B*: triplicate wells of COS-7 cells were transfected, and 2 μM iron uptake studies were performed for 2 h at pH 7.4. Error bars, SE; error bars that are not visible are smaller than the graphic.

larly tagged DMT1 plasmid transfected in parallel wells. The only difference between the two plasmids is the single-point mutation that changes the codon for amino acid 185 from glycine to arginine. In Fig. 4*B*, iron uptake studies show that the increase in uptake attributable to the G185R mutant is ~20% of the nonmutant protein. This correlates well with studies of Belgrade rat erythrocytes, where ~20% incorporation of iron into heme and ~20% utilization of iron transferrin (14) were observed.

pH dependence of human DMT1 in transfected cells vs. that of the Caco-2 enterocyte-like cell line. The apparent incongruity between the pH optimum of the DMT1 inward proton current and the duodenal brush border led us to determine the pH optimum of iron uptake in DMT1-transfected cells vs. that for the Caco-2 cell line. Caco-2 is a human colon cancer cell line with a small intestinal phenotype that has been used extensively for in vitro iron studies. The majority of the cells in this cell line assume an enterocyte-like phenotype, complete with a brush border.

Iron uptake studies from pH 5.5 to 7.5 were performed in Caco-2 and DMT1-transfected cells. The results (Fig. 5) reveal that the optimal pH of the transfected DMT1 is 6.75, which is equal to that of the Caco-2 cell line and the previously reported duodenal pH. This suggests that the inward proton current and the overall process of uptake are distinct, since the pH optima are significantly different. Additionally, this, in turn, confirms that the DMT1 protein is suitable from a pH perspective to function as the intestinal inorganic iron transporter. These studies were also performed in the human fetal intestinal epithelial cell line I-407, with peak uptake also at pH 6.75 (not shown).

Role for histidine residues in the process of DMT1 iron uptake. The pH optimum of DMT1 raised the question of a possible role for at least one histidine residue in the process of iron uptake. The acidic dissociation constant (pK_a) of histidine side chain in proteins averages 6.6, with a range of 5.5–7.0 (4, 9). Histidine side chains have been described to have pH-sensitive transport functions in proteins (3, 24) and to coordinate iron metal (20), both intriguing possibilities for this protein. Following earlier studies of other transporters, we addressed this possibility with transfected cells and chemical inactivation of histidine imidazoles using the histidine-reactive reagent DEPC (22, 24, 31, 39). Transfected cells were incubated with DEPC at increasing concentrations before iron uptake studies. The results (Fig. 6*A*) show that at low concentrations DEPC inhibited iron uptake in transfected cells. (The increased iron uptake in mock- and DMT1-transfected cells vs. that in Fig. 5 at pH 6.75 is a reproducible consequence of our treatment protocol.) Whether this effect could be inhibited by the substrate for the transporter, iron metal, was explored further. In Fig. 6*B*, cells incubated with or without 0.01 mM DEPC were used in uptake studies, with and without a nonradioactive iron metal preincubation. In Fig. 6*C*, the mean uptake from the mock transfection was subtracted from the mean COOH-terminal DMT1 uptake

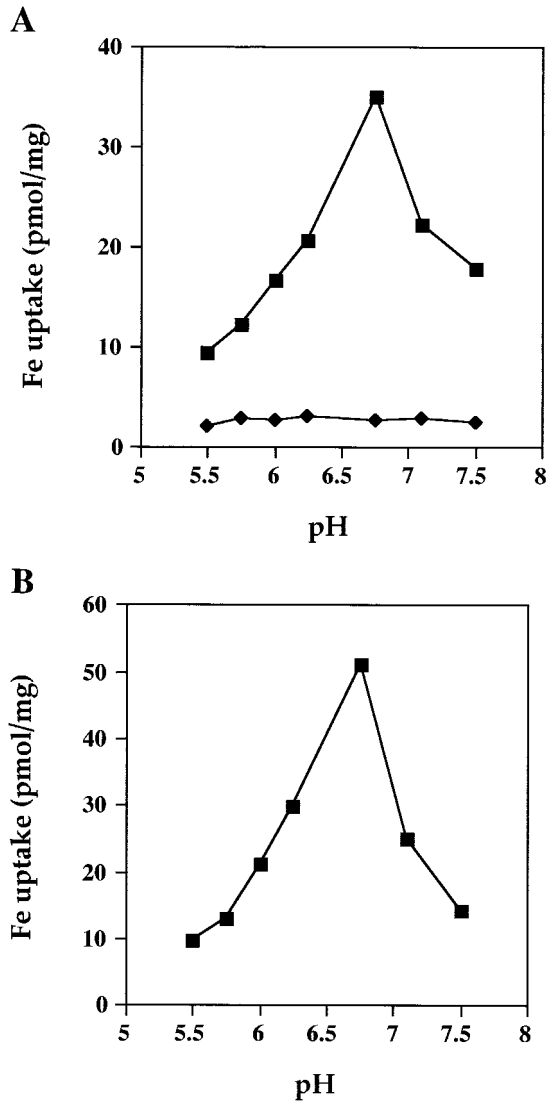

Fig. 5. pH dependence of iron transport in transfected cells and the Caco-2 enterocyte cell line. *A*: DMT1-transfected (■) and mock-transfected (◆) COS-7 cells were subjected to iron uptake studies at pH 5.5–7.5, using 2 μM radioactive iron in a 2-h incubation. *B*: Caco-2 cells incubated in the same conditions show the same pH optimum as the transfected gene. Means of triplicate experiments are plotted. Error bars (SE) at each point are smaller than the graphic.

in Fig. 6*B* to ascertain the effects of chemical modification on the function of the transgene. The cold iron preincubation inhibited the effects of DEPC inactivation of iron uptake to a level consistent with that of the cold iron metal alone. This is statistically significant by ANOVA testing by Fisher's protected least significant difference test and Scheffé's *F* test ($P < 0.0075$), suggesting a role for a functional histidine residue at the DMT1 active site.

DISCUSSION

We have explored the function of DMT1 in a transient transfection system as the candidate intestinal iron transporter, extending earlier studies to explore the physiological properties of this transporter. In-

creasing dosage of DMT1 in the COS-7 cell increases iron uptake. Since transient transfection experiments can have variable efficiency, this is an important consideration.

Our studies with increasing extracellular concentrations of iron (0–50 μM) correlate well with earlier studies in isolated enterocytes, with linear uptake with increasing iron concentration. Introduction of DMT1 into cells leads to a process that it is not saturable up to 50 μM; instead, the relationship is a straight line. This result was surprising given the previous low K_m of the proton current (15), but it conforms to the previous enterocyte studies (11, 33, 36). The linear relationship is consistent with other intestinal proteins: transporters for riboflavin and biotin have a large component to their uptake that can be modeled as diffusional (e.g., $J = V_{diff} \cdot$ [substrate], where J is flux, V_{diff} is diffusional velocity, and [substrate] is substrate concentration) (30, 31). This property allows the organism to respond to great increases in luminal substrate concentrations without saturation, increasing the effective concentration range of uptake and, therefore, the dynamic range of transport (30). The exact relationship between the proton current and iron transport will require an understanding of the mechanism of DMT1 function.

The COS-7 cell, with its ability to episomally amplify plasmid DNA containing the SV40 origin of replication, seems to be suitable to address the question of mutant DMT1 function, since the human G185R mutant was expressed comparably to the unmodified protein. Both plasmids are epitope tagged, contain the SV40 origin of replication, and differ only by the point mutation that changes glycine to arginine at *codon 185*. The use of this cell line effectively eliminates the component of reduced iron uptake attributed to lower protein expression in transfected HEK-293 cells (37), allowing functional differences to be more directly assessed. This mutation has been predicted to cause a similar human disease (18). The ~20% uptake of the G185R human DMT1 plasmid correlates very well with the 20% of inorganic iron uptake in Belgrade rat studies. These studies used the percentage of heme iron incorporation and the ability to utilize iron-loaded transferrin as measurements of functional DMT1 activity (14).

The pH optimum of uptake is equivalent for the transfected human DMT1 cDNA, the Caco-2 enterocyte-like cell line, and the previously determined pH of the human duodenum. DMT1 should therefore function very well in this environment. Iron uptake does not progressively increase with decreasing pH (increasing proton concentration), unlike the original electrophysiological description of the proton current (15). This suggests that the role of the proton current is

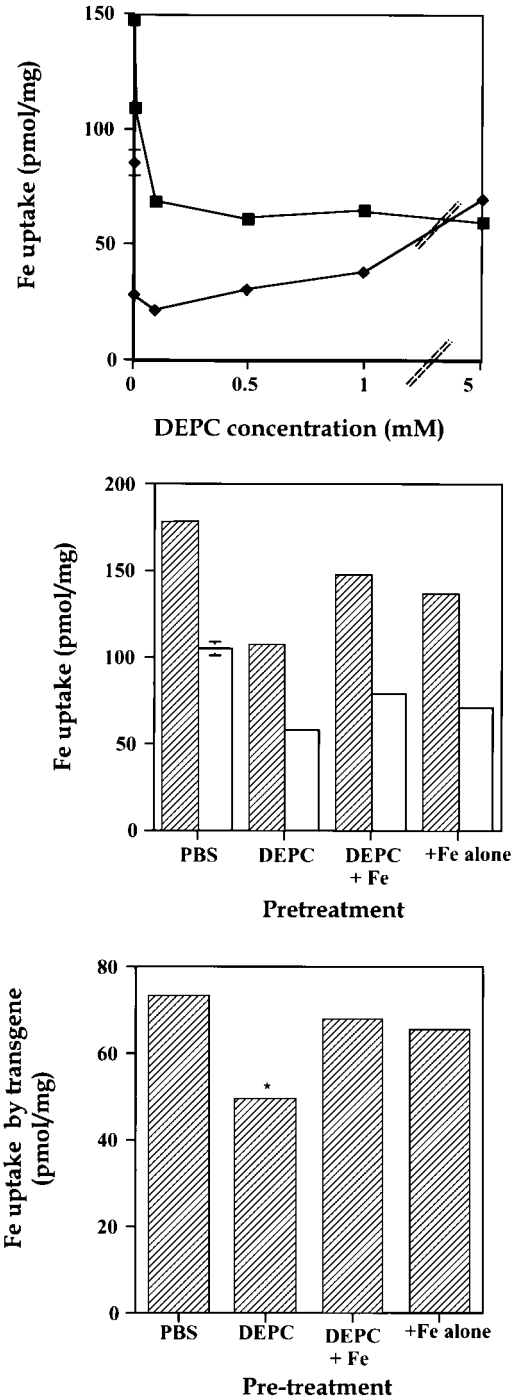

Fig. 6. Diethylpyrocarbonate (DEPC) treatment of transfected COS-7 cells at pH 6.75. Transfected cells were treated with DEPC to determine the role of a histidine side chain in iron uptake. *A*: DMT1-transfected (■) and mock-transfected (◆) cells were incubated with 0, 0.01, 0.1, 0.25, 0.5, 1, and 5 mM DEPC at room temperature for 15 min in PBS and washed with uptake buffer, and then iron uptake studies were performed using 2 μM iron at pH 6.75 for 2 h. *B*: 0.01 mM DEPC in studies of DMT1-transfected (hatched bars) and mock-transfected cells (open bars) to determine whether DEPC inhibition is prevented by iron substrate. Cells were pretreated with PBS, DEPC, DEPC + 10 μM nonradioactive $FeCl_2$ (DEPC + Fe), and 10 μM nonradioactive $FeCl_2$ alone (Fe alone), and iron uptake experiments were performed. DEPC reduction of iron uptake in DMT1-transfected cells is protected by excess cold iron to a level similar to that of iron alone, as shown in *C*, where the mean mock-transfected component has been subtracted. Error bars in *C* represent that for the DMT1 transfection alone. In each case, ANOVA is significant for the DEPC-treated cells: $^*P < 0.0075$ by Fisher's protected least significant difference test and Scheffé's F test compared with the other conditions. Error bars, SE; error bars that are not visible are smaller than the graphic.

not an electrochemical gradient driving translocation of metal ions but a more complex process. It was suggested to us that patients with gastrin-secreting tumors and, therefore, gastric acid hypersecretion have impaired iron uptake, despite a lower duodenal pH (T. Yamada, personal communication). Our pH findings for DMT1 provide a plausible mechanism for this suggestion. If the transporter is far from its optimum (>1 pH unit), the ability to transport iron metal is impaired. The ability of the duodenum to maintain the brush border near pH 6.75 to buffer the incoming gastric juice is of physiological importance in light of these findings.

The pH optimum of 6.75, coupled with the known association of the protein with an inward proton current, raised additional questions regarding the mechanism of DMT1 function. The pK_a of a free histidine side chain in proteins is ~6.6 (9), which is close to our pH optimum. This suggests a role for histidine in the transport process. The pK_a of histidine is not a fixed attribute: it can vary from 5.5 to 7.0 when buried in the core of a protein because of interactions with other residues and cofactors (4). The DEPC data support a role for at least one histidine residue at the active site, which is protected by the addition of substrate. Although the effect on uptake is incomplete, it is statistically significant ($P < 0.0075$) and is inhibited by excess substrate to a level equal to that of unlabeled substrate alone. Several factors could contribute to an incomplete effect. Chemical modification studies are limited by the accessibility of the target residue to the reagent, and a membrane-bound transporter such as DMT1 might have these residues within a membrane channel or pore. Previous studies of non-transferrin-bound iron uptake describe tight binding of the iron metal within the membrane of intestinal epithelial cells or intestinal brush-border membrane vesicles that are inaccessible to chemical chelation by relatively small compounds such as EDTA (11, 33). Finally, the protein itself has its own proton current, which might serve to protonate the histidine imidazole group; this is important, since DEPC only reacts with unprotonated histidines, potentially reducing the chemical inactivation of this side chain further (27). We consider the possible role of histidine residues in DMT1 function a preliminary finding to site-directed mutagenesis of DMT1 histidines to address this question directly. Nonetheless, from a mechanistic perspective, we find a central role for histidines in DMT1 function biochemically attractive.

Histidines can conduct proton currents on the nitrogens of the imidazole ring in terminal oxidases (17) and H^+-ATPases (22). Solvent-exposed histidine imidazole nitrogen protons are freely exchangeable (42) and have roles in other proteins as pH sensors or are responsible for pH dependence of a protein's biological effect (24). Another property of histidine residues is the ability to form coordination complexes with transition metals, including iron, by donating imidazole nitrogen lone-pair electrons to unfilled orbitals on the metal (20, 41). If DMT1 transiently coordinates iron using amino acid side chains, such as histidines and cysteines, this could explain the selectivity of the transporter for first-series transition metals rather than other divalent cations, such as Ca^{2+}. Ca^{2+} does not form complexes with the same spectrum of amino acid side chains as the first-series elements; instead, it prefers carboxylate side chains such as glutamate (23). [The converse is not necessarily true: first-series transition metalloproteins that use glutamate ligands occur, such as zinc in the active site of carboxypeptidase A (5).]

We find metal coordination in the function of this transporter attractive for a number of other reasons. It would explain the selectivity of the transporter for a particular transition metal or metals. The chemical selectivity, number, and spacing of the coordination complex are determined by the properties of the ligands and the metal (8, 20), with geometry constrained by protein structure and the chemical reactivity of the metal. All the metals transported by DMT1 (Fe^{2+}, Zn^{2+}, Mn^{2+}, Co^{2+}, Cd^{2+}, Cu^{2+}, Ni^{2+}, and Pb^{2+}) (15) readily form coordination complexes in aqueous solution, with different preferences for coordinating atoms (8). Ligand side chains such as histidines and cysteines are favored by iron complexed in ferredoxin and hemerythrin (20). Coordination would support the pH findings: if the proton current functioned as an electrochemical gradient, increasing the transmembrane gradient (lower extracellular pH) would increase uptake, as occurs in the proton-driven transport of dipolar amino acids across intestinal epithelia (40). The finding of a pH optimum suggests that some residue must be in the proper state of protonation for the process to occur. The coordination of iron by a histidine would require that one of the two histidine imidazole nitrogens be unprotonated for the metal-ligand bond to occur.

For metal coordination to be a reasonable mechanism, the role of the inward proton current would be to break a metal-protein complex by dissociating ligand-metal bonds. Although coordination complexes are a type of covalent bond, they can be weak and easily disrupted. Metal-ligand bonds are typically pH sensitive, with properties determined by the ligands and the metal involved (20).

The oxidation state of the metal can be a factor in binding and release. While iron(II) readily forms coordination complexes with lone-pair nitrogen atoms, the affinity of iron(III) for amine or imine ligands is significantly lower, with a few exceptions (notably, EDTA and 1,10-phenanthroline) (8). Valence is also a factor in sensitivity to acid disruption of these bonds. Trivalent metals lower the pK_a of coordinating ligands more than their divalent analogs, making the trivalent complexes more refractory to disruption at a given pH (20). DMT1 coordination of iron could therefore explain the observation that the preferred substrate for intestinal inorganic iron uptake is iron(II) rather than iron(III) (15, 28).

Finally, this hypothesis could explain the findings of polar iron metal entrapped within the membrane of intestinal brush-border vesicles (11, 33). Other inves-

tigators have predicted that the transmembrane segments of DMT1 and related transporters have a number of amino acid residues that are thermodynamically unfavorable to reside in a nonpolar membrane environment (1, 6). These residues are those capable of forming coordinate bonds in metalloproteins such as histidines, cysteines, aspartates, and glutamates (20). Each of these amino acids has a side chain atom that can coordinate metals and a solvent-exchangeable proton that could be used to conduct a proton current (42).

In conclusion, DMT1 in our transfection system has properties consistent with a predicted role as the intestinal iron transporter. Further studies are necessary to determine the mechanism of DMT1 function in light of known transition metal chemistry.

This work was supported by National Institute of Diabetes and Digestive and Kidney Diseases Grant DK-02501 and American Digestive Health Foundation Industry Research Scholar Award (to M. T. Worthington).

REFERENCES

1. **Agranoff D, Monahan I, Mangan J, Butcher P, and Krishna S.** *Mycobacterium tuberculosis* expresses a novel pH-dependent divalent cation transporter belonging to the Nramp family. *J Exp Med* 190: 717–724, 1999.
2. **Alvarez-Hernandez X, Smith M, and Glass J.** Regulation of iron uptake and transport by transferrin in Caco-2 cells, an intestinal cell line. *Biochim Biophys Acta* 1192: 215–222, 1994.
3. **Borza DB and Morgan WT.** Histidine-proline-rich glycoprotein as a plasma pH sensor. Modulation of its interaction with glycosaminoglycans by pH and metals. *J Biol Chem* 273: 5493–5499, 1998.
4. **Cantor CR and Sdhimmel PR.** Kinetics of ligand interactions. In: *Biophysical Chemistry. III. The Behavior of Biological Macromolecules*. San Francisco, CA: Freeman, 1980, p. 901–907.
5. **Cantor CR and Sdhimmel PR.** Structure of proteins. In: *Biophysical Chemistry: The Conformation of Biological Macromolecules*. San Francisco, CA: Freeman, 1980, p. 62.
6. **Cellier M, Prive G, Belouchi A, Kwan T, Rodrigues V, Chia W, and Gros P.** Nramp defines a family of membrane proteins. *Proc Natl Acad Sci USA* 92: 10089–10093, 1995.
7. **Chua AC and Morgan EH.** Manganese metabolism is impaired in the Belgrade laboratory rat. *J Comp Physiol [B]* 167: 361–369, 1997.
8. **Cotton FA and Wilkinson G.** *Advanced Inorganic Chemistry: A Comprehensive Text.* New York: Wiley, 1980, p. 755–760.
9. **Creighton TE.** 1.3.8 His. In: *Proteins: Structures and Molecular Properties* (2nd ed.). New York: Freeman, 1993, p. 13–14.
10. **Dorey C, Cooper C, Dickson DP, Gibson JF, Simpson RJ, and Peters TJ.** Iron speciation at physiological pH in media containing ascorbate and oxygen. *Br J Nutr* 70: 157–169, 1993.
11. **Eastham EJ, Bell JI, and Douglas AP.** Iron-transport characteristics of vesicles of brush-border and basolateral plasma membrane from the rat enterocyte. *Biochem J* 164: 289–294, 1977.
12. **Fleming MD, Trenor CC III, Su MA, Foernzler D, Beier DR, Dietrich WF, and Andrews NC.** Microcytic anaemia mice have a mutation in Nramp2, a candidate iron transporter gene. *Nat Genet* 16: 383–386, 1997.
13. **Fleming RE, Migas MC, Zhou XY, Jiang JX, Britton RS, Brunt EM, Tomatsu S, Waheed A, Bacon BR, and Sly WS.** Mechanism of increased iron absorption in murine model of hereditary hemochromatosis: increased duodenal expression of the iron transporter DMT1. *Proc Natl Acad Sci USA* 96: 3143–3148, 1999.
14. **Garrick LM, Dolan KG, Romano MA, and Garrick MD.** Non-transferrin-bound iron uptake in Belgrade and normal rat erythroid cells. *J Cell Physiol* 178: 349–358, 1999.
15. **Gunshin H, Mackenzie B, Berger UV, Gunshin Y, Romero MF, Boron WF, Nussberger S, Gollan JL, and Hediger MA.** Cloning and characterization of a mammalian proton-coupled metal-ion transporter. *Nature* 388: 482–488, 1997.
16. **Han O, Failla ML, Hill AD, Morris ER, and Smith JC Jr.** Reduction of Fe(III) is required for uptake of nonheme iron by Caco-2 cells. *J Nutr* 125: 1291–1299, 1995.
17. **Karpefors M, Adelroth P, Aagaard A, Sigurdson H, Svensson EM, and Brzezinski P.** Electron-proton interactions in terminal oxidases. *Biochim Biophys Acta* 1365: 159–169, 1998.
18. **Kishi F and Tabuchi M.** Complete nucleotide sequence of human NRAMP2 cDNA. *Mol Immunol* 34: 839–842, 1997.
19. **Lee PL, Gelbart T, West C, Halloran C, and Beutler E.** The human Nramp2 gene: characterization of the gene structure, alternative splicing, promoter region and polymorphisms. *Blood Cells Mol Dis* 24: 199–215, 1998.
20. **Lippard SJ and Berg JM.** *Principles of Bioinorganic Chemistry*. Mill Valley, CA: University Science Books, 1994, p. 2–6, 21–41.
21. **Mohan C.** *Buffers: A Guide for the Preparation and Use of Buffers in Biological Systems.* San Diego: Calbiochem-Novabiochem, 1997.
22. **Morjana NA and Scarborough GA.** Evidence for an essential histidine residue in the *Neurospora crassa* plasma membrane H^+-ATPase. *Biochim Biophys Acta* 985: 19–25, 1989.
23. **Persechini A, Moncrief ND, and Kretsinger RH.** The EF-hand family of calcium-modulated proteins. *Trends Neurosci* 12: 462–467, 1989.
24. **Pisoni RL and Velilla VQ.** Evidence for an essential histidine residue located in the binding site of the cysteine-specific lysosomal transport protein. *Biochim Biophys Acta* 1236: 23–30, 1995.
25. **Quigley EM and Turnberg LA.** Studies of luminal and mucosal pH in reflux esophagitis and antral gastritis. *Dig Dis* 10: 134–143, 1992.
26. **Rasband W.** *NIH Image* (1.62 ed.). Bethesda, MD: Natl Inst Health, 1998.
27. **Rebrin I, Thony B, Bailey SW, and Ayling JE.** Stereospecificity and catalytic function of histidine residues in 4a-hydroxytetrahydropterin dehydratase/DCoH. *Biochemistry* 37: 11246–11254, 1998.
28. **Riedel HD, Remus AJ, Fitscher BA, and Stremmel W.** Characterization and partial purification of a ferrireductase from human duodenal microvillus membranes. *Biochem J* 309: 745–748, 1995.
29. **Sadowski I and Ptashne M.** A vector for expressing GAL4(1–147) fusions in mammalian cells. *Nucleic Acids Res* 17: 7539, 1989.
30. **Said HM and Ma TY.** Mechanism of riboflavine uptake by Caco-2 human intestinal epithelial cells. *Am J Physiol Gastrointest Liver Physiol* 266: G15–G21, 1994.
31. **Said HM and Mohammadkhani R.** Involvement of histidine residues and sulfhydryl groups in the function of the biotin transport carrier of rabbit intestinal brush-border membrane. *Biochim Biophys Acta* 1107: 238–244, 1992.
32. **Savigni DL and Morgan EH.** Transport mechanisms for iron and other transition metals in rat and rabbit erythroid cells. *J Physiol (Lond)* 508: 837–850, 1998.
33. **Savin MA and Cook JD.** Iron transport by isolated rat intestinal mucosal cells. *Gastroenterology* 75: 688–694, 1978.
34. **Seebacher T and Bade EG.** Quick and easy molecular weight determination with Macintosh computers and public domain image analysis software. *Electrophoresis* 17: 1573–1574, 1996.
35. **Segel H.** Enzyme kinetics. In: *Biochemical Calculations*. New York: John Wiley & Sons, 1976, p. 214–225.
36. **Sheehan RG.** Unidirectional uptake of iron across intestinal brush border. *Am J Physiol* 231: 1438–1444, 1976.
37. **Su MA, Trenor CC, Fleming JC, Fleming MD, and Andrews NC.** The G185R mutation disrupts function of the iron transporter Nramp2. *Blood* 92: 2157–2163, 1998.
38. **Tandy S, Williams M, Leggett A, Lopez-Jimenez M, Dedes M, Ramesh B, Srai SK, and Sharp P.** Nramp2 expression is associated with pH-dependent iron uptake across the apical

membrane of human intestinal Caco-2 cells. *J Biol Chem* 275: 1023–1029, 2000.

39. **Terada T, Saito H, and Inui K.** Interaction of β-lactam antibiotics with histidine residue of rat H^+/peptide cotransporters, PEPT1 and PEPT2. *J Biol Chem* 273: 5582–5585, 1998.
40. **Thwaites DT, McEwan GT, and Simmons NL.** The role of the proton electrochemical gradient in the transepithelial absorption of amino acids by human intestinal Caco-2 cell monolayers. *J Membr Biol* 145: 245–256, 1995.
41. **Worthington MT, Amann BT, Nathans D, and Berg JM.** Metal binding properties and secondary structure of the zinc-binding domain of Nup475. *Proc Natl Acad Sci USA* 93: 13754–13759, 1996.
42. **Wuthrich K.** *NMR of Proteins and Nucleic Acids*. New York: Wiley, 1986, p. 15–19.
44. **Zoller H, Pietrangelo A, Vogel W, and Weiss G.** Duodenal metal-transporter (DMT-1, NRAMP-2) expression in patients with hereditary haemochromatosis. *Lancet* 353: 2120–2123, 1999.